JACS
JOURNAL OF THE AMERICAN CHEMICAL SOCIETY
pubs.acs.org/JACS
Article

Enantioselective Radical–Radical Cross-Couplings of β-Hydroxy Amides and *N*-Hydroxyphthalimide Esters via Ni/Photoredox Catalysis

Li-Li Zhang, Lian-Jie Li, Ning Wang, Hui Yu, and Ze-Peng Yang*

Cite This: *J. Am. Chem. Soc.* 2025, 147, 33097–33107
Read Online
ACCESS | Metrics & More | Article Recommendations | Supporting Information

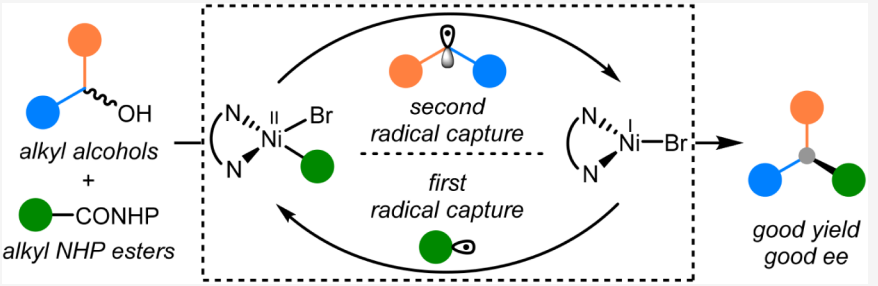

ABSTRACT: Enantioselective alkyl–alkyl cross-coupling is a powerful yet challenging strategy for constructing three-dimensional molecular architectures, which are essential in fields such as organic chemistry and pharmaceutical chemistry. While radical–radical cross-coupling offers a promising approach, achieving control over both cross- and enantioselectivity between two distinct alkyl radicals remains a formidable challenge due to their transient nature. In this article, we introduce a practical platform that combines photoredox and chiral nickel catalysis to tame transient primary and secondary alkyl radicals under mild conditions. We also present a one-pot variant wherein the *N*-hydroxyphthalimide (NHP) ester is generated in situ, enabling the streamlined synthesis of enantioenriched products in a single step from commercially available carboxylic acids and easily accessible alcohols. The utility of this method is demonstrated by diverse transformations to valuable scaffolds and bioactive molecules. A comprehensive mechanistic study has clarified the involvement of a Ni(I)/Ni(II) cycle.

INTRODUCTION

By enabling the creation of molecules with enhanced three-dimensional structural properties, enantioselective alkyl–alkyl cross-coupling serves as a powerful tool for the pharmaceutical industry.[1−3] Traditional alkyl–alkyl cross-coupling involves using an organometallic reagent as the nucleophile and an alkyl halide as the electrophile.[4−7] An appealing alternative is reductive cross-coupling, which removes reliance on organometallic species that can be sensitive to air and moisture.[8−13] In both strategies, the two alkyl species follow different mechanistic pathways: one generates a free alkyl radical in situ, while the other interacts with the transition metal catalyst through either transmetallation or oxidative addition.[14−21] This fundamental difference in reactivity ensures effective cross-selectivity between the coupling partners.

Radical–radical cross-coupling, where two distinct free radicals combine to form C–C bonds, has emerged as a promising synthetic strategy.[22,23] Unlike traditional methods, this approach bypasses functional group constraints, allowing for the coupling of diverse radical precursors (such as carboxylic acids, halides, alcohols, and others) in virtually any combination (Figure 1A).[24−27] This flexibility facilitates the efficient construction of complex molecules from simple, readily available feedstocks, paving the way for versatile and streamlined chemical synthesis. Moreover, the inherent reactivity of radicals offers key advantages, including mild reaction conditions and good functional group tolerance.[28−30] However, radical–radical couplings are typically diffusion-controlled processes, making the selective cross-coupling of two distinct transient radicals a formidable challenge in synthetic chemistry.[31] Controlling enantioselectivity at stereogenic carbon centers further exacerbates this challenge. Consequently, enantioselective radical–radical cross-coupling, especially between alkyl radicals, remains largely unexplored, with only a few successful examples reported to date.[32−42]

The persistent radical effect (PRE) is a key strategy for achieving high cross-selectivity in radical–radical couplings.[43,44] This effect operates when one radical has a

Received: June 29, 2025
Revised: August 20, 2025
Accepted: August 22, 2025
Published: August 28, 2025

https://doi.org/10.1021/jacs.5c10963
J. Am. Chem. Soc. 2025, 147, 33097–33107

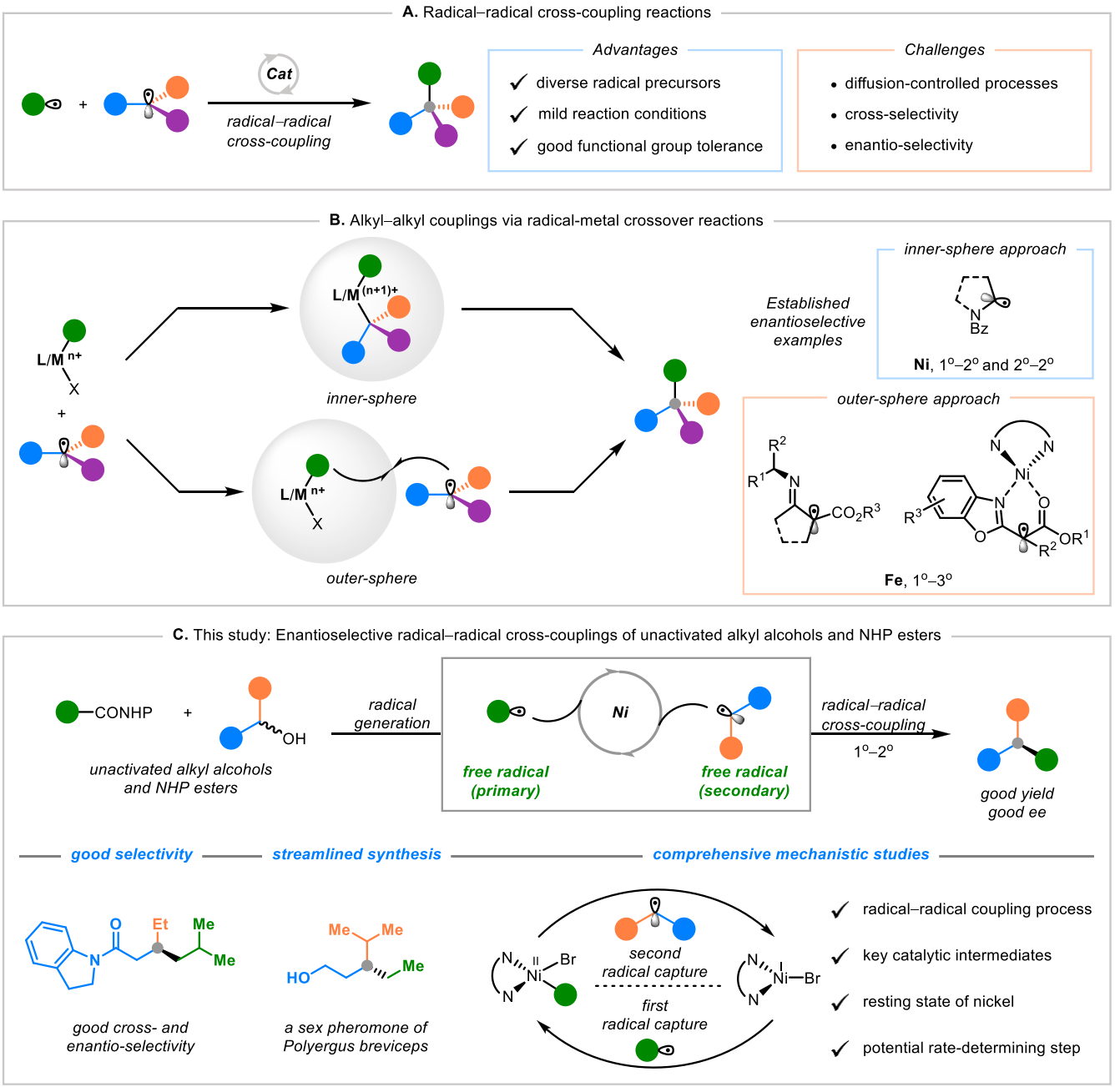

Figure 1. Background of this study. (A) The advantages and challenges of radical−radical cross-coupling reactions. (B) Alkyl−alkyl couplings via radical-metal crossover reactions. (C) This study: Enantioselective radical−radical cross-couplings of β-hydroxy amides and *N*-hydroxyphthalimide esters via Ni/photoredox catalysis.

significantly longer lifetime than its transient counterpart and both radicals are generated at equal rates. Recent research indicates that PRE applies beyond classical persistent/transient radical pairs and operates whenever considerable lifetime disparities exist. A particularly promising development in this area involves radical-metal crossover reactions, where long-lived transition-metal complexes react productively with transient radicals (Figure 1B).[45−49] In this context, transient alkyl radicals can couple with organometallic complexes through either inner-sphere reductive elimination[50−53] or outer-sphere radical substitution approaches.[54−64] However, achieving asymmetric versions of these transformations remains elusive. Notably, pioneering work by the Huo group successfully demonstrated nickel-catalyzed cross-coupling of primary/secondary and secondary/secondary alkyl radicals, with particular success in handling resonance-stabilized α-amino radicals.[65,66] Advancing this field, our group has recently introduced an iron-catalyzed system capable of coupling primary alkyl radicals with sterically demanding tertiary alkyl radicals through an outer-sphere pathway.[67,68]

Despite substantial progress in this field, the selective cross-coupling of similar alkyl radicals, especially between primary and secondary alkyl radicals derived from unactivated precursors, is still a daunting challenge. Recognizing that metal−alkyl bond strength decreases with increasing alkyl substitution,[69] we envisioned that a chiral metal catalyst could

https://doi.org/10.1021/jacs.5c10963
J. Am. Chem. Soc. 2025, 147, 33097−33107

Table 1. Enantioselective Radical–Radical Cross-Couplings of an Unactivated Alkyl NHP Ester and an Unactivated Alkyl Alcohol[abc]

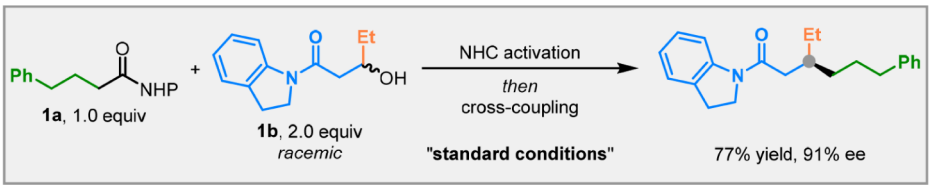

entry	variation from the "**standard conditions**"	yield (%)[a]	ee (%)[b]
1	None	77	91
2	No Ni, **PC**, Quinuclidine, or light	0	–
3	No (*S*,*S*)-**L1**	37	0
4	**L2**, instead of (*S*,*S*)-**L1**	63	60
5	**L3**, instead of (*S*,*S*)-**L1**	46	-28
6	**L4**, instead of (*S*,*S*)-**L1**	32	0
7	**L5**, instead of (*S*,*S*)-**L1**	0	–
8	**L6**, instead of (*S*,*S*)-**L1**	55	15
9	Pure $PhCF_3$	26	90
10	Pure MTBE	62	89
11	5.0 mol% $NiBr_2$•DME, 6.0 mol% (*S*,*S*)-**L1**	68	91
12	10 h, instead of 20 h	63	91
13	r.t., instead of 0 °C	23	88
14	0.05 M, instead of 0.1 M	71	90
15	3.0 mL air added (4.0 mL vial)	72	90
16	1.0 equiv H_2O added	68	80

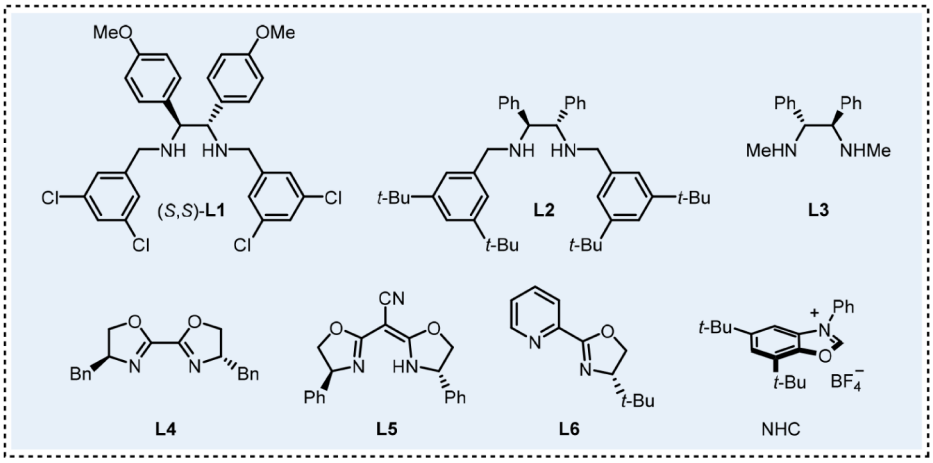

[a]Determined through GC analysis. [b]Determined through HPLC analysis. [c]Standard reaction conditions: 2.2 equiv 2,6-bis(*tert*-butyl) pyridine, 2.0 equiv NHC, $PhCF_3$, r.t., and 30 min; then 10 mol % $NiBr_2$·DME, 12 mol % (*S*,*S*)-**L1**, 1.5 mol % $(Ir[dF(CF_3)ppy]_2(dtbpy))PF_6$ (**PC**), 1.5 equiv quinuclidine, $PhCF_3$/MTBE (1/1, 0.1 M), 455 nm Blue LEDs (30 W), 0 °C, and 20 h.

preferentially stabilize the less substituted primary alkyl radical as a persistent metal–alkyl complex, thereby directing enantioselective cross-coupling with the more substituted secondary alkyl radical. Herein, we present the achievement of this objective through a dual catalytic system combining photocatalysis and chiral nickel catalysis, which effectively mediates the selective coupling between primary and secondary alkyl radicals under mild conditions, delivering coupling products with good cross- and enantioselectivity (Figure 1C). This transformation utilizes two abundant and easily accessible alkyl sources, alkyl carboxylic acids and alkyl alcohols, making it an efficient strategy for constructing bioactive molecules.[70−83] Furthermore, we present a comprehensive mechanistic investigation to clarify the underlying reaction pathway.

RESULTS AND DISCUSSION

Reaction Optimization. We began by investigating the coupling reaction between an unactivated primary alkyl *N*-hydroxyphthalimide (NHP) ester **1a** and an unactivated secondary alkyl alcohol **1b** (Table 1). After systematic optimization, we determined that using $NiBr_2$·DME in combination with the chiral diamine ligand (*S*,*S*)-**L1** effectively promotes the enantioselective radical–radical cross-coupling, yielding the desired product in 77% yield with 91% ee (entry 1). In contrast, little to no product is formed in the absence of $NiBr_2$·DME, (*S*,*S*)-**L1**, photocatalyst, quinuclidine, or light (racemic; entries 2 and 3). Screening of alternative chiral ligands indicated that (*S*,*S*)-**L1** outperforms the others (entries 4–8). We found that a mixed solvent system is more effective than using a single solvent (entries 9 and 10). Moreover, reducing the catalyst loading, shortening the reaction time, increasing the temperature (to r.t.), or lowering the concentration all lead to decreased yield (entries 11–14).

https://doi.org/10.1021/jacs.5c10963
J. Am. Chem. Soc. 2025, 147, 33097−33107

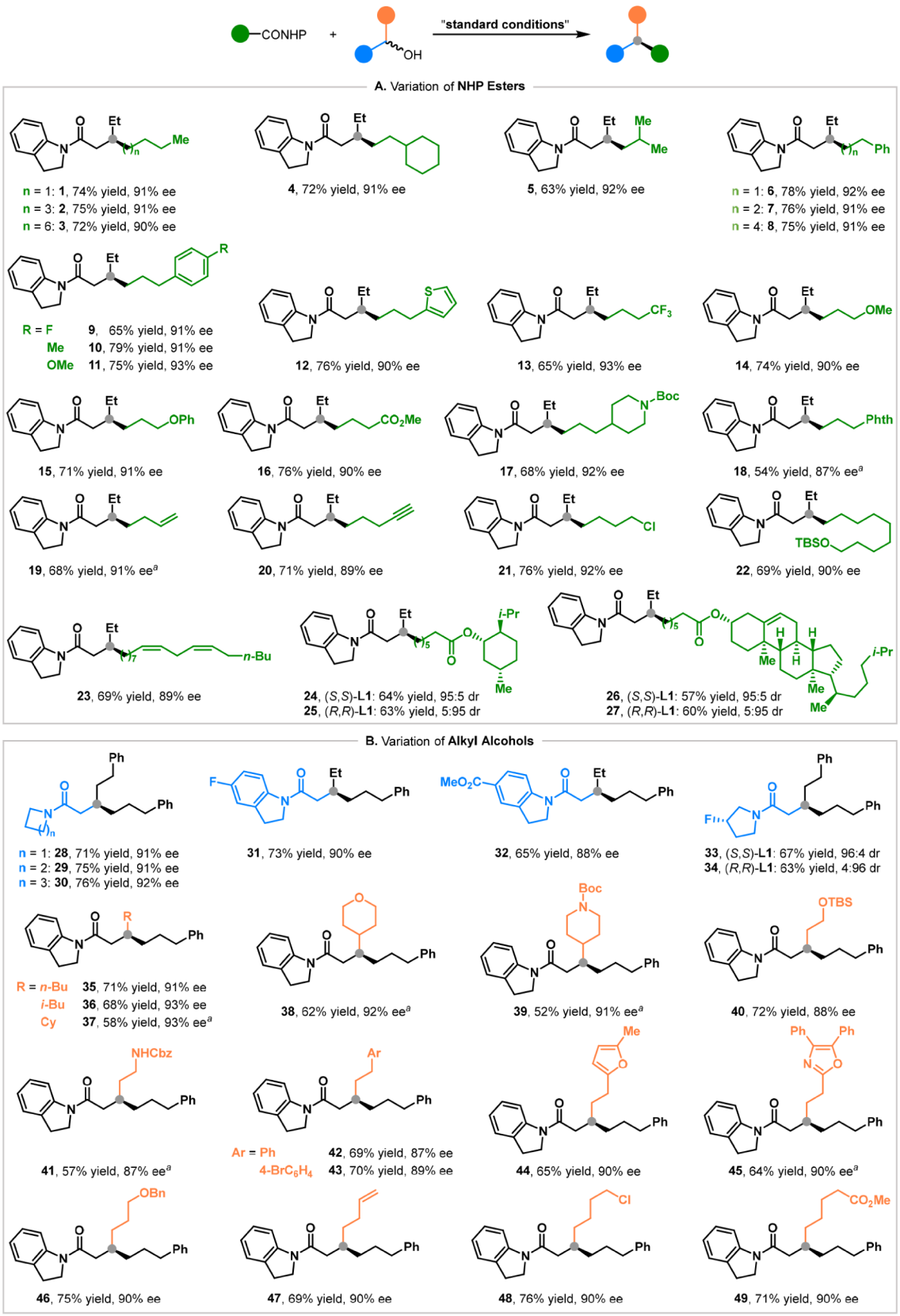

Figure 2. Scope of the catalytic enantioselective cross-coupling. All couplings were conducted on a 0.50 mmol scale (unless otherwise noted), and all yields are of purified products. (A) Variation of NHP esters. (B) Variation of alkyl alcohols. [a]The reaction was conducted for 30 h rather than 20 h.

Notably, the reaction tolerates air (entry 15), but the addition of water erodes the enantioselectivity (entry 16). The *β*-hydroxy cyclic amide substrate is essential for this reaction, as alternative substrates bearing functional groups such as −OBz,

https://doi.org/10.1021/jacs.5c10963
J. Am. Chem. Soc. 2025, 147, 33097−33107

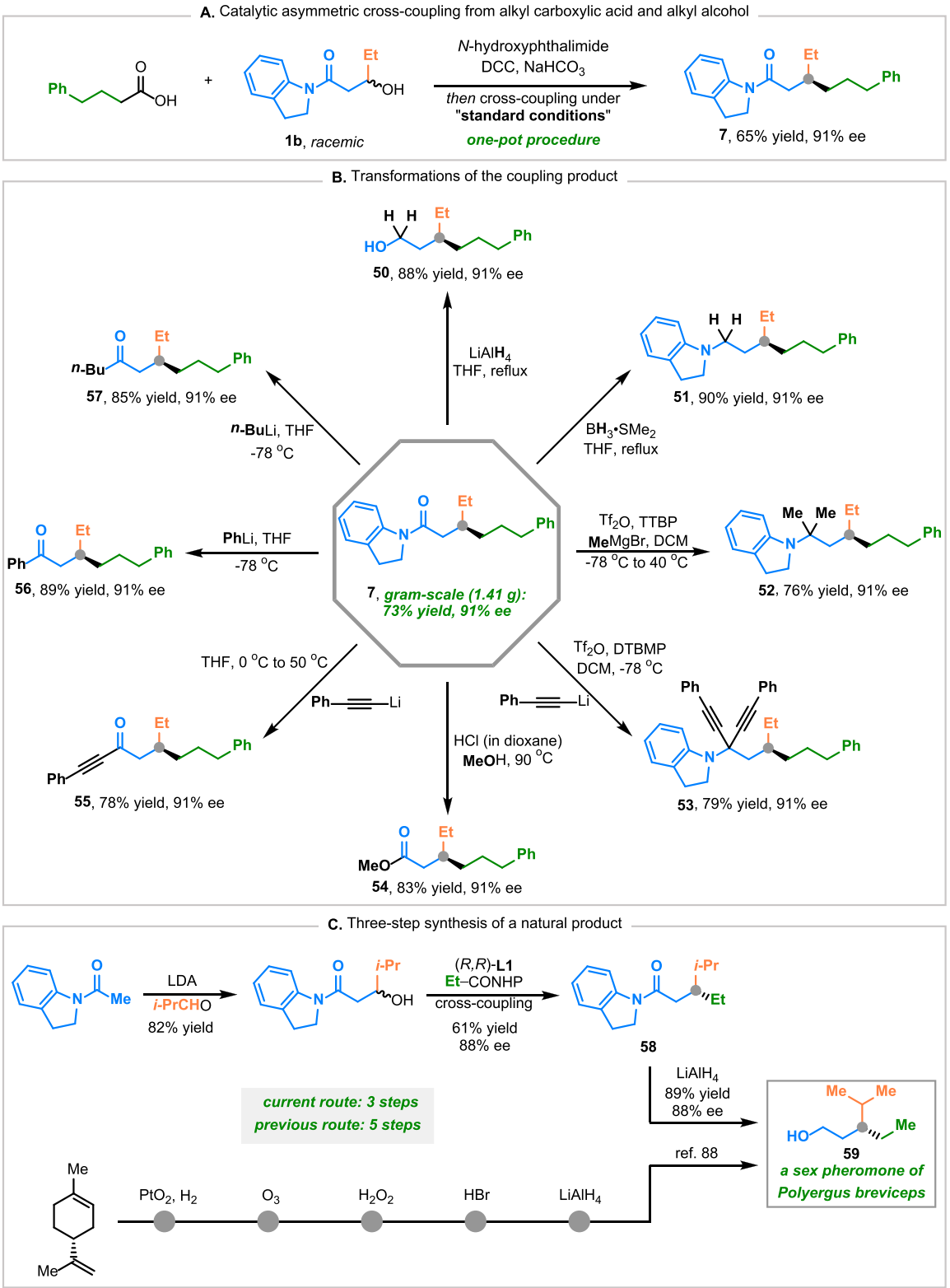

Figure 3. Applications. (A) Catalytic asymmetric cross-coupling from alkyl carboxylic acid and alkyl alcohol. Compound **1b** is added after the DCC coupling step. (B) Gram-scale reaction and transformations into other valuable enantioenriched compounds. (C) Three-step synthesis of a natural product.

−Ph, −NHCbz, −NHBoc, −NHBz, $-NPh_2$, indoline, ketone, ester, phosphonate, acyclic tertiary amide, or secondary amide, or those with modified carbon chain lengths, all fail to produce coupling products.[84] This striking selectivity highlights the critical role of the cyclic amide moiety, which likely serves as a key directing group enabling the cross-coupling reaction.

Substrate Scope. This photoinduced nickel-catalyzed system showcases remarkable versatility in constructing acyclic tertiary stereocenters through enantioselective radical−radical

https://doi.org/10.1021/jacs.5c10963
J. Am. Chem. Soc. 2025, 147, 33097−33107

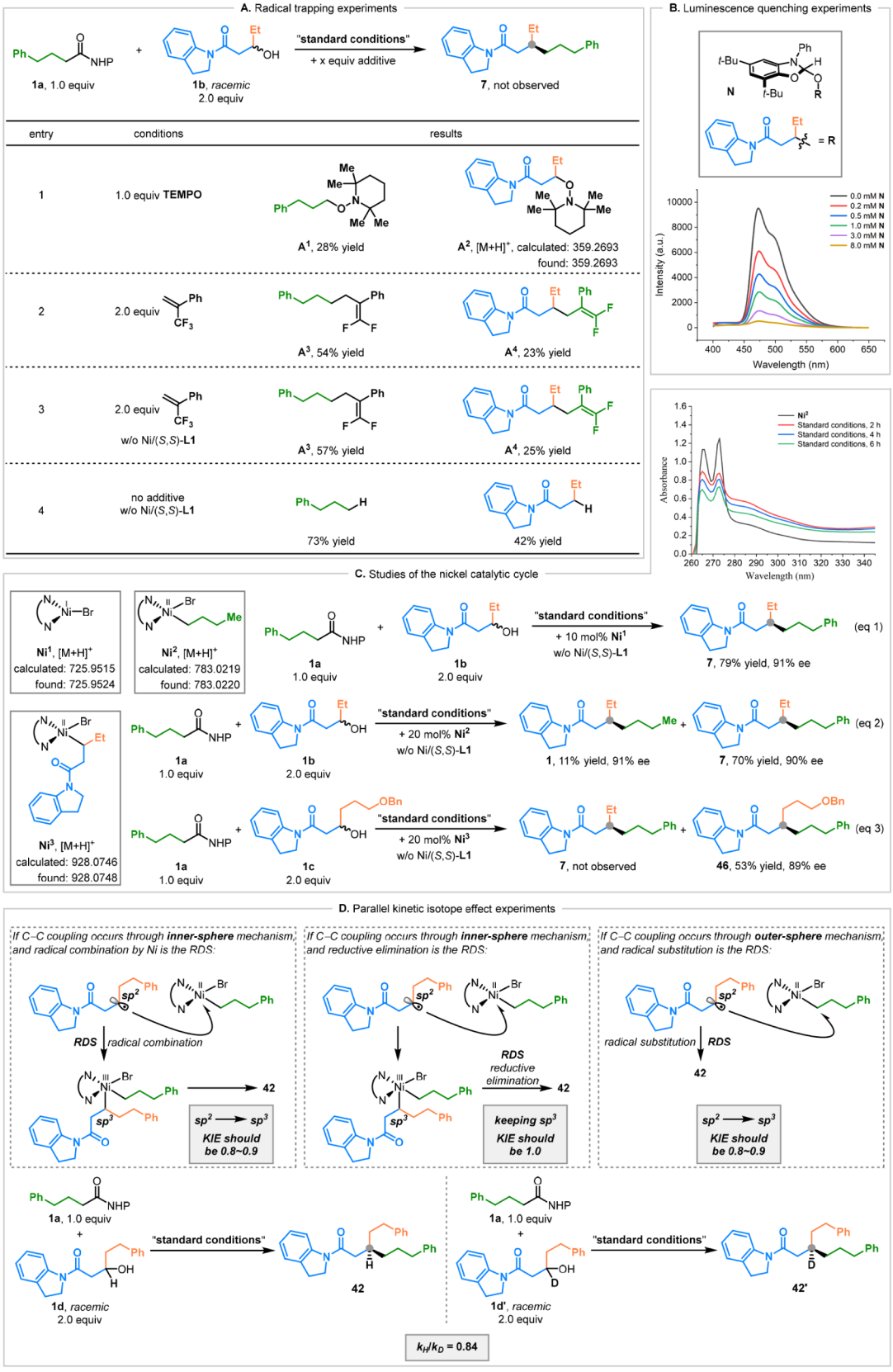

Figure 4. Mechanism. (A) Radical trapping experiments. Reaction conditions: 2.2 equiv 2,6-bis(*tert*-butyl)pyridine, 2.0 equiv NHC, $PhCF_3$, r.t., and 30 min; then 10 mol % $NiBr_2$·DME, 12 mol % (*S*,*S*)-**L1**, 1.5 mol % **PC**, 1.5 equiv quinuclidine, $PhCF_3$/MTBE (1/1, 0.1 M), additive, 455 nm Blue LEDs (30 W), 0 °C, and 20 h. The reported yields are isolated yields. (B) Luminescence quenching experiments. Conditions: **PC** (0.005 mM); (black curve) **N** (0.0 mM); (red curve) **N** (0.2 mM); (blue curve) **N** (0.5 mM); (green curve) **N** (1.0 mM); (purple curve) **N** (3.0 mM); (yellow curve) **N** (8.0 mM). (C) Mechanistic studies of the nickel catalytic cycle. UV−vis conditions: (black curve) Ni^2; (red curve) Standard

https://doi.org/10.1021/jacs.5c10963
J. Am. Chem. Soc. 2025, 147, 33097−33107

Figure 4. continued

conditions 2 h; (blue curve) Standard conditions 4 h; (green curve) Standard conditions 6 h. (D) Parallel kinetic isotope effect experiments. Rate constants were calculated using the initial rates method (<15% conversion).

cross-coupling, as demonstrated by its broad substrate scope (Figure 2). The reaction effectively couples a wide variety of unactivated primary alkyl NHP esters (Figure 2A), including both simple linear and branched alkyl groups, as well as complex substrates that contain various functional groups, such as thiophene, trifluoromethyl, ether, ester, Boc-protected amine, imide, terminal/internal alkene, terminal alkyne, unactivated primary alkyl chloride, and silyl ether, with all cases achieving high yields and good enantioselectivity (products **1**−**23**). Notably, when NHP esters with distal preexisting stereocenters are employed, the stereochemical outcome is consistently controlled by the chiral catalyst rather than the inherent chirality of the substrate (products **24**−**27**).

The reaction also exhibits good generality for unactivated secondary alkyl alcohols (β-hydroxy amides), as shown in Figure 2B. A range of cyclic tertiary amides, including one featuring a chiral fluoropyrrolidine group, can couple efficiently under the standard conditions (products **28**−**34**). Crucially, the stereochemical outcome of the products depends primarily on the chiral catalyst, with minimal influence from the stereocenters of the amide moiety. This transformation also accommodates diverse β-hydroxy amides bearing various β-alkyl substituents, ranging from *n*-butyl to more sterically demanding cyclohexyl (products **35**−**37**). Moreover, the reaction tolerates multiple functional groups including ether, Boc-protected amine, silyl ether, Cbz-protected amine, aryl bromide, furan, oxazole, terminal alkene, unactivated primary alkyl chloride, and ester, delivering the corresponding products in good yields with consistently high enantioselectivity (products **38**−**49**). The absolute configuration of products was determined by comparison with reported optical rotation data.[85]

Applications. This β-alkylation reaction can be efficiently performed as a one-pot procedure without isolation of the NHP ester, thereby enabling the synthesis of the desired products in a single step from commercially available primary alkyl carboxylic acids and easily accessible secondary alkyl alcohols (Figure 3A).[86,87]

The gram-scale synthesis (1.41 g of product) of compound **7** proceeds with yield and ee nearly identical to those obtained in the reaction conducted on a 0.50 mmol scale (Figure 3B). To highlight the synthetic versatility of this method, we have transformed **7** into various valuable enantioenriched compounds. Notably, the amide group undergoes diverse transformations with excellent retention of stereochemistry, including conversions to primary alcohol, *N*-alkyl indoline, ester, and alkynylated/arylated/alkylated ketone, all achieved in good yields.

The method's potential for converting abundant starting materials into complex molecules was further exemplified by the streamlined preparation of a natural product. Compound **59**, a sex pheromone of *Polyergus breviceps*, originally prepared in five steps from (*R*)-limonene, can now be accessed in just three steps using our approach (Figure 3C).[88]

Mechanistic Studies. To clarify the reaction mechanism, a series of mechanistic experiments were carried out. Initial radical trapping studies provided compelling evidence for the generation of two alkyl radical intermediates (Figure 4A). The reaction is completely inhibited in the presence of 1 equiv of TEMPO (2,2,6,6-tetramethyl-1-piperidinyloxy), with TEMPO-adduct $\mathbf{A^1}$ isolated in 28% yield and adduct $\mathbf{A^2}$ detected by high-resolution mass spectrometry (HR-MS) (entry 1). This radical-involving pathway was further supported by using 2 equiv of α-(trifluoromethyl)styrene as an alternative radical scavenger, which affords radical-trapping adducts $\mathbf{A^3}$ (54%) and $\mathbf{A^4}$ (23%) while completely inhibiting the productive coupling (entry 2). Notably, control experiments showed that these radical-trapping adducts can be formed in the absence of nickel catalyst (entry 3). Additional evidence for a nickel-independent radical generation pathway was observed through significant substrate consumption under nickel-free conditions, resulting in a yield of 73% for hydro-decarboxylative product and 42% for hydro-dehydroxylative product, respectively (entry 4). These collective findings indicated that the key alkyl radical species are generated through a distinct photocatalytic cycle, operating in parallel with the nickel-mediated coupling pathway. Additionally, using an α,β-unsaturated olefin instead of a β-hydroxy amide fails to produce the desired coupling product, thus ruling out the possibility of a Giese-type radical addition pathway.

Next, cyclic voltammetry (CV) studies were conducted to probe the photoredox catalytic cycle.[89] The prepared NHC-alcohol adduct **N** exhibits a half-wave potential of $E_{1/2}(\mathbf{N}^{+\bullet}/\mathbf{N})$ = +0.92 V vs saturated calomel electrode (SCE) in acetonitrile (MeCN), while substrate **1a** shows $E_p(\mathbf{1a}/\mathbf{1a}^{-\bullet})$ = −1.30 V vs SCE in MeCN (100 mV/s scan rate). Comparative analysis with the known photoredox catalyst (**PC**) potentials (for reductive quenching: $E_{1/2}(\mathbf{PC}^*/\mathbf{PC}^-)$ = +1.21 V vs SCE in MeCN; $E_{1/2}(\mathbf{PC}/\mathbf{PC}^-)$ = −1.37 V vs SCE in MeCN; for oxidative quenching: $E_{1/2}(\mathbf{PC}^+/\mathbf{PC}^*)$ = −0.89 V vs SCE in MeCN; $E_{1/2}(\mathbf{PC}^+/\mathbf{PC})$ = +1.69 V vs SCE in MeCN) reveals that while both **PC*** and $\mathbf{PC}^+$ can oxidize **N**, only $\mathbf{PC}^-$ is capable of efficiently reducing **1a**, whereas **PC*** can hardly do so (−0.89 V vs −1.30 V).[90] These electrochemical results support a reductive quenching mechanism for the photo-induced electron transfer (PET) process. This mechanistic assignment is further validated by Stern−Volmer quenching studies, which show efficient luminescence quenching of **PC*** by **N**, but negligible quenching by **1a**, consistent with the proposed reductive quenching pathway (Figure 4B).[89]

To investigate the mechanistic role of nickel intermediates in the catalytic cycle, a series of nickel complexes were synthesized and systematically evaluated. Initially, **L1**$NiBr_2$ was prepared, and its potential, along with that of **PC**, was assessed using an Ag/AgCl reference electrode ($E_{1/2}(Ni^I/Ni^0)$ = −1.84 V vs Ag/AgCl in MeCN; $E_{1/2}(\mathbf{PC}/\mathbf{PC}^-)$ = −1.37 V vs Ag/AgCl in MeCN).[89] The significant potential gap suggests that the reduction from **L1**NiBr(I) to Ni(0) by $\mathbf{PC}^-$ is thermodynamically unfavorable, implying that the catalytic cycle likely operates through Ni(I)/Ni(II) redox states rather than involving Ni(0) species.

Subsequently, three additional key nickel intermediates were synthesized: the nickel bromide complex $\mathbf{Ni^1}$, the primary alkyl−nickel bromide complex $\mathbf{Ni^2}$, and the secondary alkyl−nickel bromide complex $\mathbf{Ni^3}$, to further probe the potential role of nickel species (Figure 4C). A catalytic study employing 10

https://doi.org/10.1021/jacs.5c10963
J. Am. Chem. Soc. 2025, 147, 33097−33107

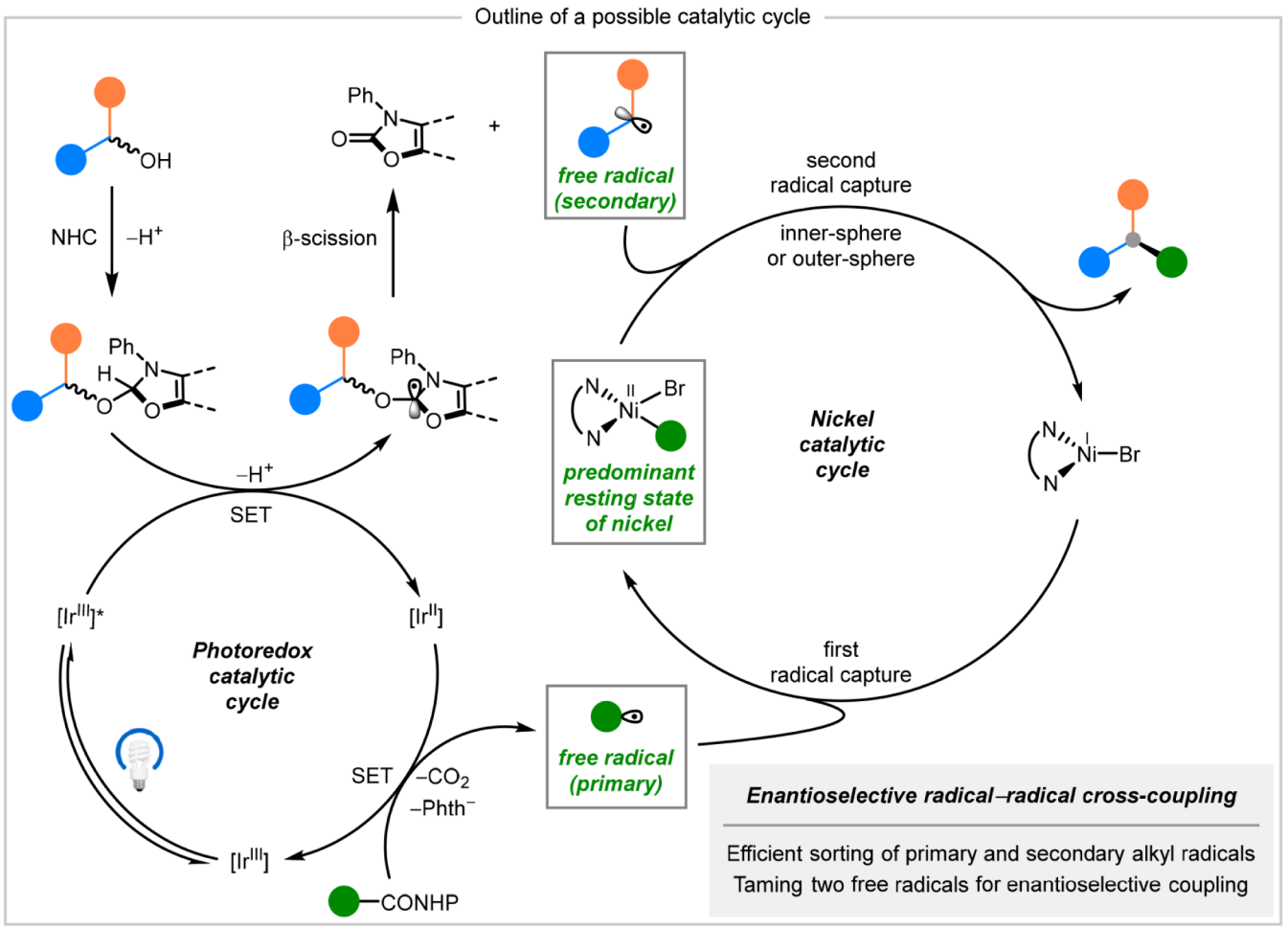

Figure 5. Outline of a possible catalytic cycle.

mol % of **Ni**^{1} affords product **7** with a yield and enantioselectivity nearly identical to those obtained in the model reaction, supporting its role as a competent catalytic intermediate (eq 1). When 20 mol % of **Ni**^{2} is employed, the coupling product **7** is obtained in 70% yield with 90% ee, comparable to the results observed in the model reaction (eq 2). Notably, the incorporation of the *n*-butyl group from **Ni**^{2} into the coupling product **1** provides direct evidence for the involvement of **Ni**^{2} in the cross-coupling reaction. In contrast, using 20 mol % of **Ni**^{3} yields only product **46** in 53% yield with 89% ee (eq 3). The absence of secondary alkyl-transfer product formation (**7**) indicates that **Ni**^{3} acts as an off-cycle species but can still reenter the catalytic pathway.[91]

Quantitative EPR analysis showed that odd-electron nickel intermediates, such as Ni(I) or Ni(III), do not accumulate to a significant extent during the reaction (<2% of the total nickel present). Furthermore, HR-MS analysis of the coupling reaction to produce compound **1** at partial conversion revealed mass consistent with **Ni**^{2}. Together with the UV−vis studies (Figure 4C, top), these results suggest that **Ni**^{2} may be the predominant resting state of the nickel catalyst during the coupling reaction.

These mechanistic insights are further substantiated by kinetic isotope effect (KIE) experiments employing *β*-deuterated substrate (Figure 4D). Three distinct mechanistic scenarios can be considered based on the proposed catalytic cycle where **Ni**^{2} serves as the resting state: (i) For an inner-sphere mechanism where radical combination by **Ni**^{2} constitutes the rate-determining step (RDS), involving sp^2 to sp^3 rehybridization, a secondary KIE (KIE = 0.8−0.9) would be expected (top left); (ii) For an inner-sphere mechanism where reductive elimination serves as the RDS without bond hybridization changes, no KIE (KIE ≈ 1.0) would be observed (top middle); (iii) For an outer-sphere mechanism with radical substitution as the RDS, a secondary KIE (KIE = 0.8−0.9) would similarly be anticipated (top right). The experimentally determined secondary KIE of 0.84 clearly demonstrates significant rehybridization during the RDS (Figure 4D, bottom); however, this observation cannot distinguish between inner-sphere and outer-sphere pathways. Additionally, these results indicate that the RDS is light-independent.[89]

Based on the above observations and previous research, a proposed catalytic cycle is depicted in Figure 5. The reaction begins with the formation of the corresponding NHC-alcohol adduct. Simultaneously, photoexcitation of the iridium photocatalyst [Ir^{III}] under blue light-emitting diodes (LEDs) generates an excited-state species [Ir^{III}]*, which undergoes single-electron transfer (SET) to produce the reduced [Ir^{II}] species while liberating a free secondary alkyl radical. The resulting [Ir^{II}] complex subsequently serves as a potent reductant, facilitating reduction of the NHP ester to generate a free primary alkyl radical. In the nickel catalytic cycle, the primary alkyl radical is initially captured by **L1**NiBr to form the primary alkyl−nickel bromide complex, identified as the

https://doi.org/10.1021/jacs.5c10963
J. Am. Chem. Soc. 2025, 147, 33097−33107

predominant resting state. Subsequent interception of the secondary alkyl radical by this Ni(II) intermediate, proceeding through either inner-sphere or outer-sphere pathways, ultimately affords the coupled product while regenerating the Ni(I) species. The radical combination (for inner-sphere mechanism) or radical substitution (for outer-sphere mechanism) is likely the RDS.

CONCLUSIONS

We have accomplished an enantioselective radical−radical cross-coupling between β-hydroxy amides and *N*-hydroxyphthalimide esters enabled by a dual Ni/photoredox catalysis. This transformation features the generation of two distinct free alkyl radicals through photoredox process, which are then selectively intercepted by a chiral diamine-ligated nickel catalyst to achieve good cross- and enantioselectivity. The reaction proceeds under mild conditions while demonstrating good functional group compatibility and scalability. The one-pot procedure offers a straightforward approach for the synthesis of complex molecules from commercially available carboxylic acids and readily accessible alkyl alcohols. The resulting enantioenriched coupling products serve as versatile synthetic building blocks, readily undergoing diverse transformations to access valuable scaffolds and bioactive molecules. Our comprehensive mechanistic studies have successfully mapped the catalytic cycle and determined the predominant nickel resting state. These investigations offer valuable guidance for future development of asymmetric radical−radical cross-coupling transformations.

ASSOCIATED CONTENT

Supporting Information

The Supporting Information is available free of charge at https://pubs.acs.org/doi/10.1021/jacs.5c10963.

Experimental details: general information, preparation of the chiral ligand, preparation of β-hydroxy amides, catalytic enantioselective cross-couplings, effect of reaction parameters, unsuccessful examples, applications, mechanistic experiments, assignments of absolute configuration, NMR spectra and determination of stereoselectivity (PDF)

AUTHOR INFORMATION

Corresponding Author

Ze-Peng Yang − *Shanghai Key Laboratory of Chemical Assessment and Sustainability, School of Chemical Science and Engineering, Tongji University, Shanghai 200092, People's Republic of China;* orcid.org/0000-0003-0248-1963; Email: zpyang@tongji.edu.cn

Authors

Li-Li Zhang − *Shanghai Key Laboratory of Chemical Assessment and Sustainability, School of Chemical Science and Engineering, Tongji University, Shanghai 200092, People's Republic of China*

Lian-Jie Li − *Shanghai Key Laboratory of Chemical Assessment and Sustainability, School of Chemical Science and Engineering, Tongji University, Shanghai 200092, People's Republic of China;* orcid.org/0009-0006-9552-1408

Ning Wang − *Shanghai Key Laboratory of Chemical Assessment and Sustainability, School of Chemical Science and Engineering, Tongji University, Shanghai 200092, People's Republic of China*

Hui Yu − *Shanghai Key Laboratory of Chemical Assessment and Sustainability, School of Chemical Science and Engineering, Tongji University, Shanghai 200092, People's Republic of China;* orcid.org/0000-0002-5717-6635

Complete contact information is available at: https://pubs.acs.org/10.1021/jacs.5c10963

Notes

The authors declare no competing financial interest.

ACKNOWLEDGMENTS

Support has been provided by the National Natural Science Foundation of China (Grant No. 22201216 to Z.-P. Y.), the National Key Research & Development Program of China (Grant No. 2023YFA1508600 to Z.-P. Y.), and the Fundamental Research Funds for the Central Universities (Grant No. 22120240079 to Z.-P. Y.).

REFERENCES

(1) Lovering, F.; Bikker, J.; Humblet, C. Escape from Flatland: Increasing Saturation as an Approach to Improving Clinical Success. *J. Med. Chem.* **2009**, *52*, 6752−6756.

(2) Lovering, F. Escape from Flatland 2: complexity and promiscuity. *Med. Chem. Commun.* **2013**, *4*, 515−519.

(3) Churcher, I.; Newbold, S.; Murray, C. W. Return to Flatland. *Nat. Rev. Chem.* **2025**, *9*, 140−141.

(4) Geist, E.; Kirschning, A.; Schmidt, T. sp^3-sp^3 Coupling reactions in the synthesis of natural products and biologically active molecules. *Nat. Prod. Rep.* **2014**, *31*, 441−448.

(5) Cherney, A. H.; Kadunce, N. T.; Reisman, S. E. Enantioselective and Enantiospecific Transition-Metal-Catalyzed Cross-Coupling Reactions of Organometallic Reagents To Construct C−C Bonds. *Chem. Rev.* **2015**, *115*, 9587−9652.

(6) Choi, J.; Fu, G. C. Transition metal−catalyzed alkyl-alkyl bond formation: Another dimension in cross-coupling chemistry. *Science* **2017**, *356* (6334), No. eaaf7230.

(7) Fu, G. C. Transition-Metal Catalysis of Nucleophilic Substitution Reactions: A Radical Alternative to S_N1 and S_N2 Processes. *ACS Cent. Sci.* **2017**, *3*, 692−700.

(8) Poremba, K. E.; Dibrell, S. E.; Reisman, S. E. Nickel-Catalyzed Enantioselective Reductive Cross-Coupling Reactions. *ACS Catal.* **2020**, *10*, 8237−8246.

(9) Pang, X.; Su, P.-F.; Shu, X.-Z. Reductive Cross-Coupling of Unreactive Electrophiles. *Acc. Chem. Res.* **2022**, *55*, 2491−2509.

(10) Ehehalt, L. E.; Beleh, O. M.; Priest, I. C.; Mouat, J. M.; Olszewski, A. K.; Ahern, B. N.; Cruz, A. R.; Chi, B. K.; Castro, A. J.; Kang, K.; Wang, J.; Weix, D. J. Cross-Electrophile Coupling: Principles, Methods, and Applications in Synthesis. *Chem. Rev.* **2024**, *124*, 13397−13569.

(11) Chen, L.-M.; Reisman, S. E. Enantioselective $C(sp^2)$−$C(sp^3)$ Bond Construction by Ni Catalysis. *Acc. Chem. Res.* **2024**, *57*, 751−762.

(12) Gong, Y.; Hu, J.; Qiu, C.; Gong, H. Insights into Recent Nickel-Catalyzed Reductive and Redox C−C Coupling of Electrophiles, $C(sp^3)$−H Bonds and Alkenes. *Acc. Chem. Res.* **2024**, *57*, 1149−1162.

(13) Xu, W.; Xu, T. Dual Nickel- and Photoredox-Catalyzed Asymmetric Reductive Cross-Couplings: Just a Change of the Reduction System? *Acc. Chem. Res.* **2024**, *57*, 1997−2011.

(14) Jones, G. D.; Martin, J. L.; McFarland, C.; Allen, O. R.; Hall, R. E.; Haley, A. D.; Brandon, R. J.; Konovalova, T.; Desrochers, P. J.; Pulay, P.; Vicic, D. A. Ligand Redox Effects in the Synthesis, Electronic Structure, and Reactivity of an Alkyl−Alkyl Cross-Coupling Catalyst. *J. Am. Chem. Soc.* **2006**, *128*, 13175−13183.

(15) Biswas, S.; Weix, D. J. Mechanism and Selectivity in Nickel-Catalyzed Cross-Electrophile Coupling of Aryl Halides with Alkyl Halides. *J. Am. Chem. Soc.* **2013**, *135*, 16192−16197.
(16) Schley, N. D.; Fu, G. C. Nickel-Catalyzed Negishi Arylations of Propargylic Bromides: A Mechanistic Investigation. *J. Am. Chem. Soc.* **2014**, *136*, 16588−16593.
(17) Weix, D. J. Methods and Mechanisms for Cross-Electrophile Coupling of Csp^2 Halides with Alkyl Electrophiles. *Acc. Chem. Res.* **2015**, *48*, 1767−1775.
(18) Diccianni, J. B.; Katigbak, J.; Hu, C.; Diao, T. Mechanistic Characterization of (Xantphos)Ni(I)-Mediated Alkyl Bromide Activation: Oxidative Addition, Electron Transfer, or Halogen-Atom Abstraction. *J. Am. Chem. Soc.* **2019**, *141*, 1788−1796.
(19) Yin, H.; Fu, G. C. Mechanistic Investigation of Enantioconvergent Kumada Reactions of Racemic α-Bromoketones Catalyzed by a Nickel/Bis(oxazoline) Complex. *J. Am. Chem. Soc.* **2019**, *141*, 15433−15440.
(20) Dawson, G. A.; Spielvogel, E. H.; Diao, T. Nickel-Catalyzed Radical Mechanisms: Informing Cross-Coupling for Synthesizing Non-Canonical Biomolecules. *Acc. Chem. Res.* **2023**, *56*, 3640−3653.
(21) Turro, R. F.; Wahlman, J. L. H.; Tong, Z. J.; Chen, X.; Yang, M.; Chen, E. P.; Hong, X.; Hadt, R. G.; Houk, K. N.; Yang, Y.-F.; Reisman, S. E. Mechanistic Investigation of Ni-Catalyzed Reductive Cross-Coupling of Alkenyl and Benzyl Electrophiles. *J. Am. Chem. Soc.* **2023**, *145*, 14705−14715.
(22) Johnson, M. D. Bimolecular homolytic displacement of transition-metal complexes from carbon. *Acc. Chem. Res.* **1983**, *16*, 343−349.
(23) Zhang, Y.; Li, K.-D.; Huang, H.-M. Bimolecular Homolytic Substitution (S_H2) at a Transition Metal. *ChemCatchem* **2024**, *16* (21), No. e202400955.
(24) Tsymbal, A. V.; Bizzini, L. D.; MacMillan, D. W. C. Nickel Catalysis via S_H2 Homolytic Substitution: The Double Decarboxylative Cross-Coupling of Aliphatic Acids. *J. Am. Chem. Soc.* **2022**, *144*, 21278−21286.
(25) Gould, C. A.; Pace, A. L.; MacMillan, D. W. C. Rapid and Modular Access to Quaternary Carbons from Tertiary Alcohols via Bimolecular Homolytic Substitution. *J. Am. Chem. Soc.* **2023**, *145*, 16330−16336.
(26) Wang, J. Z.; Lyon, W. L.; MacMillan, D. W. C. Alkene dialkylation by triple radical sorting. *Nature* **2024**, *628*, 104−109.
(27) Wang, J. Z.; Mao, E.; Nguyen, J. A.; Lyon, W. L.; MacMillan, D. W. C. Triple Radical Sorting: Aryl-Alkylation of Alkenes. *J. Am. Chem. Soc.* **2024**, *146*, 15693−15700.
(28) Twilton, J.; Le, C.; Zhang, P.; Shaw, M. H.; Evans, R. W.; MacMillan, D. W. C. The merger of transition metal and photocatalysis. *Nat. Rev. Chem.* **2017**, *1* (7), 0052.
(29) Chan, A. Y.; Perry, I. B.; Bissonnette, N. B.; Buksh, B. F.; Edwards, G. A.; Frye, L. I.; Garry, O. L.; Lavagnino, M. N.; Li, B. X.; Liang, Y.; Mao, E.; Millet, A.; Oakley, J. V.; Reed, N. L.; Sakai, H. A.; Seath, C. P.; MacMillan, D. W. C. Metallaphotoredox: The Merger of Photoredox and Transition Metal Catalysis. *Chem. Rev.* **2022**, *122*, 1485−1542.
(30) Huang, C.-Y.; Li, J.; Li, C.-J. Photocatalytic $C(sp^3)$ radical generation via C−H, C−C, and C−X bond cleavage. *Chem. Sci.* **2022**, *13*, 5465−5504.
(31) Leifert, D.; Studer, A. The Persistent Radical Effect in Organic Synthesis. *Angew. Chem., Int. Ed.* **2020**, *59*, 74−108.
(32) Uraguchi, D.; Kinoshita, N.; Kizu, T.; Ooi, T. Synergistic Catalysis of Ionic Brønsted Acid and Photosensitizer for a Redox Neutral Asymmetric α-Coupling of *N*-Arylaminomethanes with Aldimines. *J. Am. Chem. Soc.* **2015**, *137*, 13768−13771.
(33) Ma, J.; Harms, K.; Meggers, E. Enantioselective rhodium/ruthenium photoredox catalysis en route to chiral 1,2-aminoalcohols. *Chem. Commun.* **2016**, *52*, 10183−10186.
(34) Wang, C.; Qin, J.; Shen, X.; Riedel, R.; Harms, K.; Meggers, E. Asymmetric Radical−Radical Cross-Coupling through Visible-Light-Activated Iridium Catalysis. *Angew. Chem., Int. Ed.* **2016**, *55*, 685−688.
(35) Ma, J.; Rosales, A. R.; Huang, X.; Harms, K.; Riedel, R.; Wiest, O.; Meggers, E. Visible-Light-Activated Asymmetric β-C−H Functionalization of Acceptor-Substituted Ketones with 1,2-Dicarbonyl Compounds. *J. Am. Chem. Soc.* **2017**, *139*, 17245−17248.
(36) Silvi, M.; Verrier, C.; Rey, Y. P.; Buzzetti, L.; Melchiorre, P. Visible-light excitation of iminium ions enables the enantioselective catalytic β-alkylation of enals. *Nat. Chem.* **2017**, *9*, 868−873.
(37) Li, J.; Kong, M.; Qiao, B.; Lee, R.; Zhao, X.; Jiang, Z. Formal enantioconvergent substitution of alkyl halides via catalytic asymmetric photoredox radical coupling. *Nat. Commun.* **2018**, *9* (1), 2445.
(38) Mazzarella, D.; Crisenza, G. E. M.; Melchiorre, P. Asymmetric Photocatalytic C−H Functionalization of Toluene and Derivatives. *J. Am. Chem. Soc.* **2018**, *140*, 8439−8443.
(39) Li, Y.; Han, C.; Wang, Y.; Huang, X.; Zhao, X.; Qiao, B.; Jiang, Z. Catalytic Asymmetric Reductive Azaarylation of Olefins via Enantioselective Radical Coupling. *J. Am. Chem. Soc.* **2022**, *144*, 7805−7814.
(40) Byun, S.; Hwang, M. U.; Wise, H. R.; Bay, A. V.; Cheong, P. H.-Y.; Scheidt, K. A. Light-Driven Enantioselective Carbene-Catalyzed Radical-Radical Coupling. *Angew. Chem., Int. Ed.* **2023**, *62* (49), No. e202312829.
(41) Tseliou, V.; Kqiku, L.; Berger, M.; Schiel, F.; Zhou, H.; Poelarends, G. J.; Melchiorre, P. Stereospecific radical coupling with a non-natural photodecarboxylase. *Nature* **2024**, *634*, 848−854.
(42) Xu, Y.; Chen, H.; Yu, L.; Peng, X.; Zhang, J.; Xing, Z.; Bao, Y.; Liu, A.; Zhao, Y.; Tian, C.; Liang, Y.; Huang, X. A light-driven enzymatic enantioselective radical acylation. *Nature* **2024**, *625*, 74−78.
(43) Daikh, B. E.; Finke, R. G. The persistent radical effect: a prototype example of extreme, 10^5 to 1, product selectivity in a free-radical reaction involving persistent Co^{II}[macrocycle] and alkyl free radicals. *J. Am. Chem. Soc.* **1992**, *114*, 2938−2943.
(44) Fischer, H. The Persistent Radical Effect: A Principle for Selective Radical Reactions and Living Radical Polymerizations. *Chem. Rev.* **2001**, *101*, 3581−3610.
(45) Liu, W.; Lavagnino, M. N.; Gould, C. A.; Alcázar, J.; MacMillan, D. W. C. A biomimetic S_H2 cross-coupling mechanism for quaternary sp^3-carbon formation. *Science* **2021**, *374*, 1258−1263.
(46) Sakai, H. A.; MacMillan, D. W. C. Nontraditional Fragment Couplings of Alcohols and Carboxylic Acids: $C(sp^3)$−$C(sp^3)$ Cross-Coupling via Radical Sorting. *J. Am. Chem. Soc.* **2022**, *144*, 6185−6192.
(47) Mao, E.; MacMillan, D. W. C. Late-Stage $C(sp^3)$−H Methylation of Drug Molecules. *J. Am. Chem. Soc.* **2023**, *145*, 2787−2793.
(48) Yamaguchi, Y.; Hirata, Y.; Higashida, K.; Yoshino, T.; Matsunaga, S. Cobalt/Photoredox Dual-Catalyzed Cross-Radical Coupling of Alkenes via Hydrogen Atom Transfer and Homolytic Substitution. *Org. Lett.* **2024**, *26*, 4893−4897.
(49) Burton, K. I.; MacMillan, D. W. C. Rapid access to 3-substituted bicyclo[1.1.1]pentanes. *Chem* **2025**, *11* (5), 102587.
(50) Yang, B.; Wang, X.-Y.; Huang, X.-T.; Liu, Z.-Y.; Li, X.; Huang, T.; Li, X.-S.; Wu, L.-Z.; Fang, R.; Liu, Q. Visible-Light-Mediated Two Transient $C(sp^3)$ Radical-Selective Cross-Coupling via Nickel Catalyst Continuous Capture: Synthesis of Pyrroline Derivatives. *ACS Catal.* **2023**, *13*, 15331−15339.
(51) Li, C.; Cheng, J.; Wan, X.; Li, J.; Zu, W.; Xu, Y.; Huang, Y.; Huo, H. Ni/Photoredox-Catalyzed Enantioselective Acylation of α-Bromobenzoates with Aldehydes: A Formal Approach to Aldehyde-Aldehyde Cross-Coupling. *J. Am. Chem. Soc.* **2024**, *146*, 19909−19918.
(52) Li, P.; Zhu, Z.; Guo, C.; Kou, G.; Wang, S.; Xie, P.; Ma, D.; Feng, T.; Wang, Y.; Qiu, Y. Nickel-electrocatalysed $C(sp^3)$−$C(sp^3)$ cross-coupling of unactivated alkyl halides. *Nat. Catal.* **2024**, *7*, 412−421.
(53) Ling, B.; Yao, S.; Ouyang, S.; Bai, H.; Zhai, X.; Zhu, C.; Li, W.; Xie, J. Nickel-Catalyzed Highly Selective Radical C−C Coupling from Carboxylic Acids with Photoredox Catalysis. *Angew. Chem., Int. Ed.* **2024**, *63* (32), No. e202405866.

(54) Gan, X.-C.; Kotesova, S.; Castanedo, A.; Green, S. A.; Møller, S. L. B.; Shenvi, R. A. Iron-Catalyzed Hydrobenzylation: Stereoselective Synthesis of (−)-Eugenial C. *J. Am. Chem. Soc.* **2023**, *145*, 15714−15720.
(55) Gan, X.-C.; Zhang, B.; Dao, N.; Bi, C.; Pokle, M.; Kan, L.; Collins, M. R.; Tyrol, C. C.; Bolduc, P. N.; Nicastri, M.; Kawamata, Y.; Baran, P. S.; Shenvi, R. Carbon quaternization of redox active esters and olefins by decarboxylative coupling. *Science* **2024**, *384*, 113−118.
(56) Chen, R.; Intermaggio, N. E.; Xie, J.; Rossi-Ashton, J. A.; Gould, C. A.; Martin, R. T.; Alcázar, J.; MacMillan, D. W. C. Alcohol-alcohol cross-coupling enabled by S_H2 radical sorting. *Science* **2024**, *383*, 1350−1357.
(57) Tan, T.-D.; Serviano, J. M. I.; Luo, X.; Qian, P.-C.; Holland, P. L.; Zhang, X.; Koh, M. J. Congested C(sp^3)−rich architectures enabled by iron-catalysed conjunctive alkylation. *Nat. Catal.* **2024**, *7*, 321−329.
(58) Kong, L.; Gan, X.-C.; van der Puyl Lovett, V. A.; Shenvi, R. A. Alkene Hydrobenzylation by a Single Catalyst That Mediates Iterative Outer-Sphere Steps. *J. Am. Chem. Soc.* **2024**, *146*, 2351−2357.
(59) Cong, F.; Sun, G.-Q.; Ye, S.-H.; Hu, R.; Rao, W.; Koh, M. J. A Bimolecular Homolytic Substitution-Enabled Platform for Multicomponent Cross-Coupling of Unactivated Alkenes. *J. Am. Chem. Soc.* **2024**, *146*, 10274−10280.
(60) Cai, Q.; McWhinnie, I. M.; Dow, N. W.; Chan, A. Y.; MacMillan, D. W. C. Engaging Alkenes in Metallaphotoredox: A Triple Catalytic, Radical Sorting Approach to Olefin-Alcohol Cross-Coupling. *J. Am. Chem. Soc.* **2024**, *146*, 12300−12309.
(61) Pace, A. L.; Xu, F.; Liu, W.; Lavagnino, M. N.; MacMillan, D. W. C. Iron-Catalyzed Cross-Electrophile Coupling for the Formation of All-Carbon Quaternary Centers. *J. Am. Chem. Soc.* **2024**, *146*, 32925−32932.
(62) Zhang, Q.; Wu, S.; Wu, X. Iron/photoredox dual-catalyzed redox-neutral double decarboxylative C(sp^3)−C(sp^3) cross-coupling. *Green Chem.* **2024**, *26*, 11334−11339.
(63) Fang, T.-Y.; Jiang, M.-Y.; Zheng, M.-M.; Ma, J.-A.; Zhang, F.-G. S_H2 Decarboxylative Monofluoromethylation of Aliphatic Carboxylic Acids Enabled by Nickel/Photoredox Dual Catalysis. *Angew. Chem., Int. Ed.* **2025**, *64* (32), No. e202507632.
(64) Lyon, W. L.; Wang, J. Z.; Alcázar, J.; MacMillan, D. W. C. Aminoalkylation of Alkenes Enabled by Triple Radical Sorting. *J. Am. Chem. Soc.* **2025**, *147*, 2296−2302.
(65) Li, J.; Cheng, B.; Shu, X.; Xu, Z.; Li, C.; Huo, H. Enantioselective alkylation of α-amino C(sp^3)−H bonds via photoredox and nickel catalysis. *Nat. Catal.* **2024**, *7*, 889−899.
(66) Li, T.; Xu, Z.; Huang, Y.; Zu, W.; Huo, H. Enantioselective Alkyl−Acyl Radical Cross-Coupling Enabled by Metallaphotoredox Catalysis. *J. Am. Chem. Soc.* **2025**, *147*, 10999−11009.
(67) Li, L.-J.; Zhang, J.-C.; Li, W.-P.; Zhang, D.; Duanmu, K.; Yu, H.; Ping, Q.; Yang, Z.-P. Enantioselective Construction of Quaternary Stereocenters via Cooperative Photoredox/Fe/Chiral Primary Amine Triple Catalysis. *J. Am. Chem. Soc.* **2024**, *146*, 9404−9412.
(68) Li, L.-J.; Zhang, J.-C.; Tang, J.-Y.; Yu, H.; Yang, Z.-P. Acyclic Quaternary Stereocenters via Catalytic Asymmetric Cross-Couplings with Unactivated Alkyl *N*-Hydroxyphthalimide Esters. *Angew. Chem., Int. Ed.* **2025**, *64* (24), No. e202506883.
(69) Simoes, J. A. M.; Beauchamp, J. L. Transition metal-hydrogen and metal-carbon bond strengths: the keys to catalysis. *Chem. Rev.* **1990**, *90*, 629−688.
(70) Johnston, C. P.; Smith, R. T.; Allmendinger, S.; MacMillan, D. W. C. Metallaphotoredox-catalysed sp^3−sp^3 cross-coupling of carboxylic acids with alkyl halides. *Nature* **2016**, *536*, 322−325.
(71) Qin, T.; Cornella, J.; Li, C.; Malins, L. R.; Edwards, J. T.; Kawamura, S.; Maxwell, B. D.; Eastgate, M. D.; Baran, P. S. A general alkyl-alkyl cross-coupling enabled by redox-active esters and alkylzinc reagents. *Science* **2016**, *352*, 801−805.
(72) Zuo, Z.; Cong, H.; Li, W.; Choi, J.; Fu, G. C.; MacMillan, D. W. C. Enantioselective Decarboxylative Arylation of α-Amino Acids via the Merger of Photoredox and Nickel Catalysis. *J. Am. Chem. Soc.* **2016**, *138*, 1832−1835.
(73) Cornella, J.; Edwards, J. T.; Qin, T.; Kawamura, S.; Wang, J.; Pan, C.-M.; Gianatassio, R.; Schmidt, M.; Eastgate, M. D.; Baran, P. S. Practical Ni-Catalyzed Aryl−Alkyl Cross-Coupling of Secondary Redox-Active Esters. *J. Am. Chem. Soc.* **2016**, *138*, 2174−2177.
(74) Wang, D.; Zhu, N.; Chen, P.; Lin, Z.; Liu, G. Enantioselective Decarboxylative Cyanation Employing Cooperative Photoredox Catalysis and Copper Catalysis. *J. Am. Chem. Soc.* **2017**, *139*, 15632−15635.
(75) Dong, Z.; MacMillan, D. W. C. Metallaphotoredox-enabled deoxygenative arylation of alcohols. *Nature* **2021**, *598*, 451−456.
(76) Cheng, L.; Lin, Q.; Chen, Y.; Gong, H. Recent Progress on Transition-Metal-Mediated Reductive C(sp^3)-O Bond Radical Addition and Coupling Reactions. *Synthesis* **2022**, *54*, 4426−4446.
(77) Anwar, K.; Merkens, K.; Troyano, F. J. A.; Gómez-Suárez, A. Radical Deoxyfunctionalisation Strategies. *Eur. J. Org. Chem.* **2022**, *2022* (26), No. e202200330.
(78) Beil, S. B.; Chen, T. Q.; Intermaggio, N. E.; MacMillan, D. W. C. Carboxylic Acids as Adaptive Functional Groups in Metallaphotoredox Catalysis. *Acc. Chem. Res.* **2022**, *55*, 3481−3494.
(79) Pang, X.; Shu, X.-Z. Reductive Deoxygenative Functionalization of Alcohols by First Row Transition Metal Catalysis. *Chin. J. Chem.* **2023**, *41*, 1637−1652.
(80) Mandal, T.; Mallick, S.; Islam, M.; De Sarkar, S. Alcohols as Alkyl Synthons Enabled by Photoredox-Catalyzed Deoxygenative Activation. *ACS Catal.* **2024**, *14*, 13451−13496.
(81) Zhang, L.-L.; Gao, Y.-Z.; Cai, S.-H.; Yu, H.; Shen, S.-J.; Ping, Q.; Yang, Z.-P. Ni-catalyzed enantioconvergent deoxygenative reductive cross-coupling of unactivated alkyl alcohols and aryl bromides. *Nat. Commun.* **2024**, *15* (1), 2733.
(82) Zeng, H.; Yin, R.; Zhao, Y.; Ma, J.-A.; Wu, J. Modular alkene synthesis from carboxylic acids, alcohols and alkanes via integrated photocatalysis. *Nat. Chem.* **2024**, *16*, 1822−1830.
(83) Zhang, L.-L.; Gao, Y.-Z.; Wang, N.; Yu, H.; Shen, S.-J.; Duanmu, K.; Yang, Z.-P. Enantioconvergent deoxygenative reductive cross-coupling of lactic acid derivatives. *Sci. China: Chem., 68*, 2025.
(84) For a broad exploration of other potential substrates, see **Figure S7** of the Supporting Information.
(85) For details, please see section IX of the Supporting Information.
(86) Edwards, J. T.; Merchant, R. R.; McClymont, K. S.; Knouse, K. W.; Qin, T.; Malins, L. R.; Vokits, B.; Shaw, S. A.; Bao, D.-H.; Wei, F.-L.; Zhou, T.; Eastgate, M. D.; Baran, P. S.; et al. Decarboxylative alkenylation. *Nature* **2017**, *545* (7653), 213−219.
(87) Yang, Z.-P.; Freas, D. J.; Fu, G. C. The Asymmetric Synthesis of Amines via Nickel-Catalyzed Enantioconvergent Substitution Reactions. *J. Am. Chem. Soc.* **2021**, *143*, 2930−2937.
(88) Greenberg, L.; Tröger, A. G.; Francke, W.; McElfresh, J. S.; Topoff, H.; Aliabadi, A.; Millar, J. G. Queen Sex Pheromone of the Slave-making Ant, Polyergus breviceps. *J. Chem. Ecol.* **2007**, *33*, 935−945.
(89) For details, please see section VIII of the Supporting Information.
(90) Corrigan, N.; Shanmugam, S.; Xu, J.; Boyer, C. Photocatalysis in organic and polymer synthesis. *Chem. Soc. Rev.* **2016**, *45*, 6165−6212.
(91) 1-(Indolin-1-yl)pentan-1-one is generated in 11% yield (based on **1a**), accounting for the secondary alkyl group's fate in **Ni^3**.

https://doi.org/10.1021/jacs.5c10963
J. Am. Chem. Soc. 2025, 147, 33097−33107